Wrinkling of Wide Sandwich Panels/Beams With Orthotropic Phases by an Elasticity Approach

G. A. Kardomateas
Professor of Aerospace Engineering
Fellow ASME
Georgia Institute of Technology,
Atlanta, GA 30332-0150

There exist many formulas for the critical compression of sandwich plates, each based on a specific set of assumptions and a specific plate or beam model. It is not easy to determine the accuracy and range of validity of these rather simple formulas unless an elasticity solution exists. In this paper, we present an elasticity solution to the problem of buckling of sandwich beams or wide sandwich panels subjected to axially compressive loading (along the short side). The emphasis on this study is on the wrinkling (multi-wave) mode. The sandwich section is symmetric and all constituent phases, i.e., the facings and the core, are assumed to be orthotropic. First, the pre-buckling elasticity solution for the compressed sandwich structure is derived. Subsequently, the buckling problem is formulated as an eigen-boundary-value problem for differential equations, with the axial load being the eigenvalue. For a given configuration, two cases, namely symmetric and anti-symmetric buckling, are considered separately, and the one that dominates is accordingly determined. The complication in the sandwich construction arises due to the existence of additional "internal" conditions at the face sheet/core interfaces. Results are produced first for isotropic phases (for which the simple formulas in the literature hold) and for different ratios of face-sheet vs core modulus and face-sheet vs core thickness. The results are compared with the different wrinkling formulas in the literature, as well as with the Euler buckling load and the Euler buckling load with transverse shear correction. Subsequently, results are produced for one or both phases being orthotropic, namely a typical sandwich made of glass/polyester or graphite/epoxy faces and polymeric foam or glass/phenolic honeycomb core. The solution presented herein provides a means of accurately assessing the limitations of simplifying analyses in predicting wrinkling and global buckling in wide sandwich panels/beams.
[DOI: 10.1115/1.1978919]

1 Introduction

The compressive strength of thin sheets can be realized only if they are stabilized against buckling. In sandwich construction, two such sheets (face-sheets) are bonded to a core slab of different (light) material. Both the core and the face-sheets can be isotropic or anisotropic.

Panels of this construction give rise to a set of problems of strength, stiffness, and stability analogous to, but by no means identical with, the well-known problems of ordinary homogeneous elastic beam/plates. One of these is "cylindrical buckling." Referring to Fig. 1, the panel is so wide that lines along the y axis can be taken as uncarved. Therefore, a unit width can be treated as an Euler column. Buckling is either like column buckling (Euler buckling) or a short wave "wrinkling" of the face sheets. In the former, the core may exhibit a substantial shearing deformation; in the latter, it acts like an elastic foundation and the buckling deformation is mainly confined to the layers adjacent to the face sheets.

Wrinkling of a symmetric configuration can occur in a symmetric mode or an antisymmetric one (Fig. 2). The initial investigations of this mode of buckling were by Hoff and Mautner [1], Goodier and Neou [2] and Gough, Elam, and de Bruyne [3]. Based on these early investigations, a whole chapter is devoted to wrinkling in Allen's book [4]. Recently, interest has also been in wrinkling under biaxial loading (Birman and Bert [5]).

The existence of different wrinkling formulas based on various beam or plate models underscores the need for an elasticity solution, in order to compare the accuracy of the predictions from the simple beam/plate formulas. Elasticity solutions for buckling have become available mainly for the axisymmetric cylindrical shell geometry, due to the availability of three-dimensional elasticity solutions for the pre-buckling state and the ease of formulation afforded by the axisymmetry. In particular, Kardomateas [6] and Kardomateas and Chung [7] formulated and solved the problem for the case of uniform external pressure and orthotropic homogeneous material (a two-dimensional "ring" assumption was made in the first paper). Homogeneous cylindrical shells under axial compression were studied by Kardomateas [8,9] and by Soldatos and Ye [10] for combined axial compression and uniform external pressure (the latter was based on a successive approximation method).

As far as sandwich structures, a three-dimensional elasticity solution for the buckling of a sandwich long shell under external pressure (again, "ring" assumption) was recently done by Kardomateas and Simitses [11]. In all these studies, a pre-requisite to obtaining elasticity solutions for shell buckling is the existence of three-dimensional elasticity solutions to the pre-buckling problem. For the monolithic homogeneous cylindrical shells, the elasticity solutions for orthotropy provided by Lekhnitskii [12] were used, whereas for the sandwich shells, the elasticity solution of Kardomateas [13] was used.

In this paper we again make the simplifying assumption of a two-dimensional problem by considering a wide plate. Because the plate is wide, lines along the long dimension can be taken as uncurved during buckling and the problem reduces to two-

Contributed by the Applied Mechanics Division of The American Society of Mechanical Engineers for publication in the ASME Journal of Applied Mechanics. Manuscript received by the Applied Mechanics Division, February 11, 2003; final revision, November 4, 2004. Associate Editor. K. Ravi-Chandar. Discussion on the paper should be addressed to the Editor, Prof. Robert M. McMeeking, Journal of Applied Mechanics, Department of Mechanical and Environmental Engineering, University of California - Santa Barbara, Santa Barbara, CA 93106-5070, and will be accepted until four months after final publication in the paper itself in the ASME Journal of Applied Mechanics.

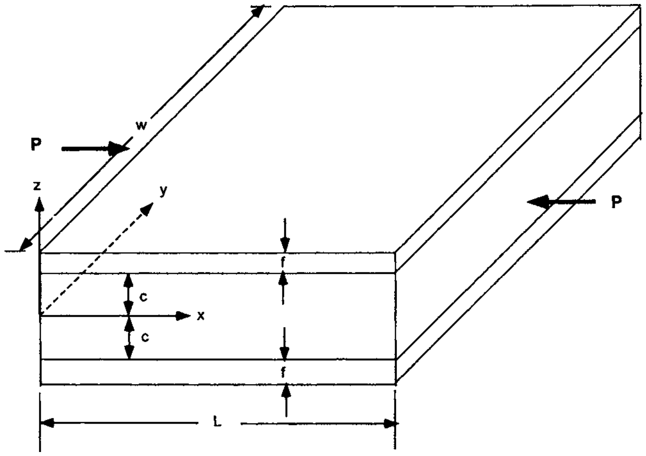

Fig. 1 Definition of the geometry for a sandwich wide panel/beam under axial compression

dimensional (equivalent to a beam rather than a plate assumption). This assumption would also allow for a direct comparison with the wrinkling formulas that exist in the literature.

In the beginning, the elasticity solution for the pre-buckling state is derived for the case of a sandwich plate with generally orthotropic phases under axial loading. Subsequently, the governing buckling equations along with the corresponding boundary conditions are derived. These reduce to an eigen-boundary value problem for differential equations with the axial load being the eigenvalue. The complication in the sandwich construction arises due to the existence of additional "internal" conditions at the face sheet/core interfaces. The shooting method is used to solve the problem thus formulated.

2 Formulation

By considering the equations of equilibrium in terms of the second Piola-Kirchhoff stress tensor, subtracting these at the perturbed and initial conditions, and making order of magnitude assumptions on the products of stresses and strains/rotations, based on the fact that a characteristic feature of stability problems is the shift from positions with small rotations to positions with rotations substantially exceeding the strains, the buckling equations for a Cartesian coordinate system can be obtained (Novozhilov [14]):

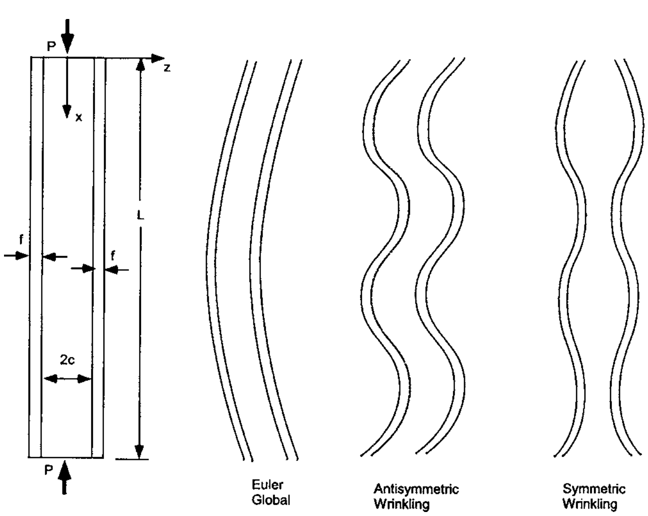

Fig. 2 Buckling modes

$$\frac{\partial}{\partial x}(\sigma_{xx} - \tau^0_{xy}\omega_z + \tau^0_{xz}\omega_y) + \frac{\partial}{\partial y}(\tau_{xy} - \sigma^0_{yy}\omega_z + \tau^0_{yz}\omega_y) + \frac{\partial}{\partial z}(\tau_{xz} + \sigma^0_{zz}\omega_y - \tau^0_{yz}\omega_z) = 0, \tag{1a}$$

$$\frac{\partial}{\partial x}(\tau_{xy} + \sigma^0_{xx}\omega_z - \tau^0_{xz}\omega_x) + \frac{\partial}{\partial y}(\sigma_{yy} - \tau^0_{yz}\omega_x + \tau^0_{xy}\omega_z) + \frac{\partial}{\partial z}(\tau_{yz} - \sigma^0_{zz}\omega_x + \tau^0_{xz}\omega_z) = 0, \tag{1b}$$

$$\frac{\partial}{\partial x}(\tau_{xz} - \sigma^0_{xx}\omega_y + \tau^0_{xy}\omega_x) + \frac{\partial}{\partial y}(\tau_{yz} + \sigma^0_{yy}\omega_x - \tau^0_{xy}\omega_y) + \frac{\partial}{\partial z}(\sigma_{zz} - \tau^0_{xz}\omega_y + \tau^0_{yz}\omega_x) = 0. \tag{1c}$$

In the previous equations, σ^0_{ij} are the values of stresses at the initial equilibrium position (pre-buckling state), and σ_{ij} and ω_j are the values of stresses and rotations at the perturbed position (buckled state).

The boundary conditions associated with Eq. (1) can be obtained from the traction (stress resultant) relationships in terms of the second Piola-Kirchhoff stress tensor, and in the general case of an external hydrostatic pressure loading (in which case the magnitude of the surface load remains invariant under deformation, but its direction changes). By writing these equations for the initial and the perturbed equilibrium position and then subtracting them and using the previous arguments on the relative magnitudes of the rotations, the following boundary conditions on a surface which has outward unit normal $(\hat{l},\hat{m},\hat{n})$ and is under the action of a hydrostatic pressure, p, are obtained [14]:

$$(\sigma_{xx} - \tau^0_{xy}\omega_z + \tau^0_{xz}\omega_y)\hat{l} + (\tau_{xy} - \sigma^0_{yy}\omega_z + \tau^0_{yz}\omega_y)\hat{m} + (\tau_{xz} + \sigma^0_{zz}\omega_y - \tau^0_{yz}\omega_z)\hat{n} = p(\omega_z\hat{m} - \omega_y\hat{n}), \tag{2a}$$

$$(\tau_{xy} + \sigma^0_{xx}\omega_z - \tau^0_{xz}\omega_x)\hat{l} + (\sigma_{yy} - \tau^0_{yz}\omega_x + \tau^0_{xy}\omega_z)\hat{m} + (\tau_{yz} - \sigma^0_{zz}\omega_x + \tau^0_{xz}\omega_z)\hat{n} = p(\omega_x\hat{n} - \omega_z\hat{l}), \tag{2b}$$

$$(\tau_{xz} - \sigma^0_{xx}\omega_y + \tau^0_{xy}\omega_x)\hat{l} + (\tau_{yz} + \sigma^0_{yy}\omega_x - \tau^0_{xy}\omega_y)\hat{m} + (\sigma_{zz} - \tau^0_{xz}\omega_y + \tau^0_{yz}\omega_x)\hat{n} = p(\omega_y\hat{l} - \omega_x\hat{m}). \tag{2c}$$

For the bounding surfaces, $\hat{l}=\hat{m}=0$ and $\hat{n}=\pm 1$. These conditions will also be used when we impose traction continuity at the core/face sheet interfaces.

2.1 Pre-buckling State. Let us assume general orthotropy for the face sheet, $i=f$, or the core, $i=c$:

$$\begin{bmatrix} \sigma^{(i)}_{xx} \\ \sigma^{(i)}_{yy} \\ \sigma^{(i)}_{zz} \\ \tau^{(i)}_{yz} \\ \tau^{(i)}_{xz} \\ \tau^{(i)}_{xy} \end{bmatrix} = \begin{bmatrix} c^i_{11} & c^i_{12} & c^i_{13} & 0 & 0 & 0 \\ c^i_{12} & c^i_{22} & c^i_{23} & 0 & 0 & 0 \\ c^i_{13} & c^i_{23} & c^i_{33} & 0 & 0 & 0 \\ 0 & 0 & 0 & c^i_{44} & 0 & 0 \\ 0 & 0 & 0 & 0 & c^i_{55} & 0 \\ 0 & 0 & 0 & 0 & 0 & c^i_{66} \end{bmatrix} \begin{bmatrix} \epsilon^{(i)}_{xx} \\ \epsilon^{(i)}_{yy} \\ \epsilon^{(i)}_{zz} \\ \gamma^{(i)}_{yz} \\ \gamma^{(i)}_{xz} \\ \gamma^{(i)}_{xy} \end{bmatrix} \quad (i=f,c) \tag{3}$$

where c^i_{kl} are the stiffness constants (we have used the notation $1 \equiv x, 2 \equiv y, 3 \equiv z$, see Fig. 1).

Assuming a pre-buckling displacement field in the form:

$$u_0 = Pd_1 x; \quad v_0 = Pd_2 y; \quad w_0 = P\left(d_3\frac{z^3}{3} + d_4 z\right), \tag{4a}$$

would satisfy the displacement continuity conditions at face-sheet/core interfaces and the symmetry conditions.

Substituting into the strain-displacement and then stress-strain relations (3), leads to zero shear strains and stresses:

$$\tau_{xy}^0=\tau_{xz}^0=\tau_{yz}^0=0, \tag{4b}$$

and normal pre-buckling stresses in the form (for $i=f,c$):

$$\sigma_{xx}^{0(i)}=P[c_{11}^i d_1+c_{12}^i d_2+c_{13}^i(d_3 z^2+d_4)], \tag{4c}$$

$$\sigma_{yy}^{0(i)}=P[c_{12}^i d_1+c_{22}^i d_2+c_{23}^i(d_3 z^2+d_4)], \tag{4d}$$

$$\sigma_{zz}^{0(i)}=P[c_{13}^i d_1+c_{23}^i d_2+c_{33}^i(d_3 z^2+d_4)]. \tag{4e}$$

Notice that it is easily seen that the stresses in Eqs. (4*b*)–(4*e*) produce no resultant moment. The constants d_1, d_2, d_3, and d_4 can be found as follows.

First, the condition of zero tractions at the bounding surfaces, $\sigma_{zz}=0$, i.e., at $z=\pm(c+f)$, gives

$$c_{13}^f d_1+c_{23}^f d_2+c_{33}^f[d_3(c+f)^2+d_4]=0. \tag{4f}$$

Second, the condition of zero resultant force on the bounding sides normal to the y axis, $\int\sigma_{yy}w\,dz=0$, at $y=0,w$, gives

$$\left(c_{12}^f f+c_{12}^c c\right)d_1+\left(c_{22}^f f+c_{22}^c c\right)d_2+\left\{c_{23}^f[(c+f)^3-c^3]+c_{23}^c c^3\right\}\frac{d_3}{3}+\left(c_{23}^f f+c_{23}^c c\right)d_4=0. \tag{4g}$$

Third, the condition of the resultant applied compressive load, P, on the bounding sides normal to the x axis, $\int\sigma_{xx}w\,dz=-P$, i.e., at $x=0,L$, gives

$$\left(c_{11}^f f+c_{11}^c c\right)d_1+\left(c_{12}^f f+c_{12}^c c\right)d_2+\left\{c_{13}^f[(c+f)^3-c^3]+c_{13}^c c^3\right\}\frac{d_3}{3}+\left(c_{13}^f f+c_{13}^c c\right)d_4=-\frac{1}{2w}. \tag{4h}$$

Finally, traction continuity at the face-sheet/core interface, i.e., at $z=\pm c$, requires $\sigma_{zz}^c=\sigma_{zz}^f$, i.e., the fourth condition:

$$c_{13}^f d_1+c_{23}^f d_2+c_{33}^f(d_3 c^2+d_4)=c_{13}^c d_1+c_{23}^c d_2+c_{33}^c(d_3 c^2+d_4). \tag{4i}$$

Therefore, there are four linear algebraic equations, Eqs. (4*f*)–(4*i*), which can be used to determine the four unknowns, d_1, d_2, d_3, and d_4.

Notice that if the phases are isotropic, with Young's modulus, E_i and Poisson's ratio ν_i then,

$$c_{11}^i=c_{22}^i=c_{33}^i=\frac{1-\nu_i}{(1-2\nu_i)(1+\nu_i)}E_i, \tag{4j}$$

$$c_{12}^i=c_{13}^i=c_{23}^i=\frac{\nu_i}{(1-2\nu_i)(1+\nu_i)}E_i \tag{4k}$$

2.2 Perturbed State. The buckling equations (1) can be written in terms of the buckling displacemenis u, v, and w by using the strain vs displacement relations:

$$\epsilon_{xx}=u_{,x},\quad \epsilon_{yy}=v_{,y},\quad \epsilon_{zz}=w_{,z}, \tag{5a}$$

$$\gamma_{xy}=u_{,y}+v_{,x},\quad \gamma_{xz}=u_{,z}+w_{,x},\quad \gamma_{yz}=v_{,z}+w_{,y}, \tag{5b}$$

and rotation vs displacement relations:

$$2\omega_x=w_{,y}-v_{,z},\quad 2\omega_y=u_{,z}-w_{,x},\quad 2\omega_z=v_{,x}-u_{,y}, \tag{5c}$$

and then using the stress-strain relations (3). The following three equations are obtained for zero pre-buckling shear stresses. These equations apply at every point through the thickness, but for convenience we have dropped the superscript i,

$$c_{11}u_{,xx}+\left(c_{66}-\frac{\sigma_{yy}^0}{2}\right)u_{,yy}+\left(c_{55}+\frac{\sigma_{zz}^0}{2}\right)u_{,zz}+\left(c_{12}+c_{66}-\frac{\sigma_{yy}^0}{2}\right)v_{,xy}+\left(c_{13}+c_{55}-\frac{\sigma_{zz}^0}{2}\right)w_{,xz}+\frac{\sigma_{zz,z}^0}{2}(u_{,z}-w_{,x})=0, \tag{6a}$$

$$c_{22}v_{,yy}+\left(c_{66}+\frac{\sigma_{xx}^0}{2}\right)v_{,xx}+\left(c_{44}+\frac{\sigma_{zz}^0}{2}\right)v_{,zz}+\left(c_{12}+c_{66}-\frac{\sigma_{xx}^0}{2}\right)u_{,xy}+\left(c_{44}+c_{23}-\frac{\sigma_{zz}^0}{2}\right)w_{,yz}+\frac{\sigma_{zz,z}^0}{2}(v_{,z}-w_{,y})=0, \tag{6b}$$

$$c_{33}w_{,zz}+\left(c_{55}+\frac{\sigma_{xx}^0}{2}\right)w_{,xx}+\left(c_{44}+\frac{\sigma_{yy}^0}{2}\right)w_{,yy}+\left(c_{13}+c_{55}-\frac{\sigma_{xx}^0}{2}\right)u_{,xz}+\left(c_{44}+c_{23}-\frac{\sigma_{yy}^0}{2}\right)v_{,yz}=0. \tag{6c}$$

The corresponding from Eqs. (2*a*)–(2*c*) traction boundary conditions at the bounding surfaces for $\hat{l}=\hat{m}=0$ and $\hat{n}=1$ are

$$\left(c_{55}+\frac{\sigma_{zz}^0}{2}\right)u_{,z}+\left(c_{55}-\frac{\sigma_{zz}^0}{2}\right)w_{,x}=0, \tag{7a}$$

$$\left(c_{44}-\frac{\sigma_{zz}^0}{2}\right)w_{,y}+\left(c_{44}+\frac{\sigma_{zz}^0}{2}\right)v_{,z}=0, \tag{7b}$$

$$c_{13}u_{,x}+c_{23}v_{,y}+c_{33}w_{,z}=0 \tag{7c}$$

In the petrurbed position we seek two-dimensional equilibrium modes as follows:

$$u_i=U_i(z)\cos\lambda x;\quad v_i=0;\quad w_i=W_i(z)\sin\lambda x,\quad \lambda=\frac{m\pi}{L}\quad i=f,c \tag{8}$$

Substituting into Eq. (7), results in the following two linear homogeneous ordinary differential equations of the second order for $U_i(z), W_i(z)$, where $i=c$ for $0\leqslant z\leqslant c$ and $i=f$ for $c\leqslant z\leqslant(c+f)$:

$$\left(c_{55}^{(i)}+\frac{\sigma_{zz}^{0(i)}}{2}\right)U_i''+\frac{\sigma_{zz,z}^{0(i)}}{2}U_i'-c_{11}^{(i)}\lambda^2U_i+\left(c_{13}^{(i)}+c_{55}^{(i)}-\frac{\sigma_{zz}^{0(i)}}{2}\right)\lambda W_i'-\frac{\sigma_{zz,z}^{0(i)}}{2}\lambda W_i=0, \tag{9a}$$

and

$$c_{33}^{(i)}W_i''-\left(c_{55}^{(i)}+\frac{\sigma_{xx}^{0(i)}}{2}\right)\lambda^2W_i-\left(c_{13}^{(i)}+c_{55}^{(i)}-\frac{\sigma_{xx}^{0(i)}}{2}\right)\lambda U_i'=0. \tag{9b}$$

The associated boundary conditions are as follows.

(a) At the bounding surfaces, $z=c+f$, we have the following two traction-free conditions:

$$c_{55}^{(f)}U_f'+c_{55}^{(f)}\lambda W_f=0, \tag{10a}$$

$$c_{33}^{(f)}W_f'-c_{13}^{(f)}\lambda U_f=0 \tag{10b}$$

(b) At the face-sheet/core interface, $z=c$, we have the following four conditions at each of the interfaces.

Displacement continuity:

$$U_f=U_c;\quad W_f=W_c. \tag{10c}$$

Traction continuity:

$$\left(c_{55}^{(f)}+\frac{\sigma_{zz}^0}{2}\right)U_f'+\left(c_{55}^{(f)}-\frac{\sigma_{zz}^0}{2}\right)\lambda W_f=\left(c_{55}^{(c)}+\frac{\sigma_{zz}^0}{2}\right)U_c'+\left(c_{55}^{(c)}-\frac{\sigma_{zz}^0}{2}\right)\lambda W_c, \tag{10d}$$

$$c_{33}^{(f)}W_f' - c_{13}^{(f)}\lambda U_f = c_{33}^{(c)}W_c' - c_{13}^{(c)}\lambda U_c. \tag{10e}$$

(c) At the axis of symmetry, $z=0$, we have the following conditions.

For symmetric wrinkling:

$$U_c' = W_c = 0, \text{ symmetric wrinkling} \tag{10f}$$

For antisymmetric wrinkling:

$$U_c = W_c' = 0, \text{ antisymmetric wrinkling} \tag{10g}$$

Notice that since the construction is assumed to be symmetric, only half of the sandwich needs to be considered.

Solution of the eigen-boundary-value problem for differential equations. Equations (9) and (10) constitute an eigenvalue problem for differential equations, with the axial load, P, the parameter (two point boundary value problem). An important point is that the pre-buckling stresses $\sigma_{jj}^{0(i)}(z)$, depend *linearly* on the applied axial load, P (the parameter), through expressions in the form of Eq. (4) and this makes possible the direct application of standard solution techniques.

With respect to the method used there is a difference between the present problem and the homogeneous orthotropic body (apart from being shell geometry) solved by Kardomateas [6]. The complication in the present problem is due to the fact that the displacement field is continuous but has a slope discontinuity at the face-sheet/core interfaces. This is the reason that the displacement field was not defined as one function but as two distinct functions for $i=f$, and $i=c$, i.e., the face sheet and the core. Our formulation of the problem employs, hence, "internal" boundary conditions at the face-sheet/core interface, as outlined earlier. Due to this complication, the shooting method (Press et al. [15]) was deemed to be the best way to solve this eigen-boundary-value problem for differential equations. A special version of the shooting method was formulated and programmed for this problem. In fact, for each of the two constituent phases of the sandwich structure, we have five variables: $y_1=U_i, y_2=U_i', y_3=W_i, y_4=W_i'$, and $y_5=P$. The five differential equations are: $y_1'=y_2$, the first equilibrium equation (9*a*), $y_3'=y_4$, the second equilibrium equation (9*b*) and $y_5'=0$.

The method starts from the middle of the core, $z=0$ and integrates the five first-order differential equations from $z=0$ to the face-sheet/core interface $z=c$ (i.e., through the core). At the start point, $z=0$, we have three conditions as follows:

(a) for symmetric wrinkling: $U_c'=y_2=0, W_c=y_3=0$ and a third condition of (abritrarily) setting $U_c=y_1=1.0$, therefore we have two freely specifiable variables, the $P=y_5$ and the $W_c'=y_4$.

(b) for antisymmetric wrinkling: $U_c=y_1=0, W_c'=y_4=0$ and a third condition of (abritrarily) setting $W_c=y_3=1.0$, therefore we have two freely specifiable variables, the $P=y_5$ and the $U_c'=y_2$.

The freely specifiable starting values at $z=0$ are taken as the values from the simple plate/beam theory solutions available in the literature (described later).

Once we reach the face-sheet/core interface, $z=c$, the tractions from the core side are calculated; these should equal the tractions from the face-sheet side, according to the internal boundary conditions on the face-sheet/core interface, Eqs. (10*d*) and (10*e*). This allows finding the slopes of the displacements, $y_2=U_f'$ and $y_4=W_f'$ for starting the shooting into the face-sheet [notice that the other three functions, $y_1=U_f, y_3=W_f$ and $y_5=P$ are continuous according to Eq. (10*c*), and their values at $z=c$ have already been found at the end of the integration step through the core]. The next step is integrating the five differential equations from $z=c$ to $z=c+f$, i.e., through the face-sheet. Once the outer bounding surface, $z=c+f$, is reached, the traction boundary conditions, Eqs. (10*a*) and (10*b*), are imposed. Multi-dimensional Newton-Raphson is then used to develop a linear matrix equation for the two increments to the adjustable parameters, which are the y_5 and y_4 at $z=0$ for the case of symmetric wrinkling, and the the y_5 and y_2 at $z=0$ for the case of antisymmetric wrinkling. These increments are solved for and added and the shooting repeats until convergence. For the integration phase, we used a Runge-Kutta driver with adaptive step size control. The method produced results very fast and without any numerical complication.

As has already been stated, in the numerical scheme, the starting point (guess) is one of the simple formulas in the literature; in particular, we have used Allen's [4] solution; therefore, we input the Allen's [4] solution as a guess and then obtain the elasticity solution by the shooting method described; this is done for a range of m's, around Allen's critical m. Therefore, we vary m in the range of ±20 of the Allen's critical m (of course, the lower bound for m is $m=1$) and obtain the corresponding load; the critical m is the one that results in the lowest load (critical value).

Furthermore, for the integration phase we use a Runge-Kutta driver with monitoring of local truncation error to ensure accuracy and adjust step size; the initial step size to be attempted is 1/20th of the corresponding thickness (core or face sheet) and the numerical tolerance is 5×10^{-6}. A finer initial step size or tolerance has indicated absolutely no effect on the solution.

3 Plate/Beam Wrinkling Formulas in the Literature, Results and Discussion

Several formulas can be found in the literature for the critical wrinkling load. Allen's book [4] devotes a whole chapter on the problem. A simple formula can be found in this book for the critical stress for isotropic core and face-sheet. Allen's formula [4] is based on a beam differential equation for the face sheet, assumed to be supported by an elastic medium (the core), which extends infinitely on one side of the beam (hence the face is unaffected by the opposing face):

$$\sigma_{f,cr} = B_1 E_f^{1/3} E_c^{2/3}; \text{ where } B_1 = 3[12(3-\nu_c)^2(1+\nu_c)^2]^{-1/3}, \tag{11a}$$

$$\left(\frac{m\pi f}{L}\right)_{cr} = \frac{\pi}{C}\left(\frac{E_f}{E_c}\right)^{-1/3}; \quad \text{where } C = \pi[(3-\nu_c)(1+\nu_c)/12]^{1/3}. \tag{11b}$$

Goodier and Neou [2] give the following formula for isotropic core with $\nu_c=0$ and face-sheet with $\nu_f=1/3$, where $\rho=E_f/E_c$.

$$\frac{\sigma_{f,cr}}{E_f} = 0.655\rho^{-2/3}\left(1+\frac{0.51\rho^{1/3}+0.32}{\rho^{2/3}+0.39}\right), \quad \text{and } \left(\frac{m\pi f}{2L}\right)_{cr} = 0.726\rho^{-1/3}. \tag{11c}$$

Hoff and Mautner [1] give the following simple formula:

$$\sigma_{f,cr} = 0.91(E_f E_c G_c)^{1/3}; \quad \left(\frac{m\pi f}{L}\right)_{cr} = \frac{\pi}{1.65}E_f^{-1/3}(E_c G_c)^{1/6}. \tag{11d}$$

Although variations of this formula can be developed depending on symmetric or antisymmetric cases and also for thinner cores, Hoff and Mautner [1] concluded from their analysis that the very simple formula of Eq. (11*d*) is a conservative estimate of the critical load for all cases.

Although there are other formulas in the literature, such as Plantema's [16], there seem to introduce only small variations and the aforementioned three formulas will be taken herein as representative and compared with. In particular, Plantema's [16] critical load is:

$$\sigma_{f,cr} = \frac{0.825}{\sqrt[3]{1-\nu_f^2}}\sqrt[3]{E_f E_c G_c}. \tag{11e}$$

Table 1 Critical loads for E_f/E_c=1,000. Loads normalized with the Euler load (w/o shear), Eq. (12*a*) *W*=wrinkling (multi-wave); *GL*=global (Euler).

f/h	$\tilde{P}_{Elast}$ (m) (% difference from elasticity)	$\tilde{P}^{W}_{Allen}$ (m)	$\tilde{P}^{W}_{Goodier}$ (m)	$\tilde{P}^{W}_{Hoff}$ (m)	$\tilde{P}^{GL}_{Allen}$
0.01 Antisymm	0.07381 (24) (W)	0.06724 (25) (−8.9%)	0.07368 (23) (−0.2%)	0.07709 (27) (+4.4%)	0.2021 (+173.8%)
0.02 Antisymm	0.07393 (12) (W)	0.06753 (13) (−8.7%)	0.07400 (12) (+0.1%)	0.07742 (13) (+4.7%)	0.1156 (+56.4%)
0.03 Antisymm	0.07288 (7) (W)	0.06854 (8) (−6.0%)	0.07511 (8) (+3.1%)	0.07859 (9) (+7.8%)	0.08199 (+12.5%)
0.04 Antisymm	0.06489 (1) (GL)	0.06977 (6) (+7.5%)	0.07646 (6) (+17.8%)	0.07999 (7) (+23.3%)	0.06414 (−1.2%)
0.05 Antisymm	0.05411 (1) (GL)	0.07110 (5) (+31.4%)	0.07792 (5) (+44.0%)	0.08152 (5) (+50.7%)	0.05310 (−1.9%)

Table 2 Critical loads for E_f/E_c=500. Loads normalized with the Euler load (w/o shear), Eq. (12*a*) *W*=wrinkling (multi-wave); *GL*=global (Euler).

f/h	$\tilde{P}_{Elast}$ (m) (% difference from elasticity)	$\tilde{P}^{W}_{Allen}$ (m)	$\tilde{P}^{W}_{Goodier}$ (m)	$\tilde{P}^{W}_{Hoff}$ (m)	$\tilde{P}^{GL}_{Allen}$
0.01 Antisymm	0.1222 (30) (W)	0.1100 (32) (−10.0%)	0.1222 (29) (0%)	0.1261 (34) (+3.2%)	0.3302 (+170.2%)
0.02 Antisymm	0.1210 (15) (W)	0.1089 (16) (−10.0%)	0.1210 (15) (0%)	0.1248 (17) (+3.1%)	0.2056 (+69.4%)
0.03 Antisymm	0.1211 (10) (W)	0.1099 (11) (−9.2%)	0.1222 (10) (+0.9%)	0.1261 (11) (+4.1%)	0.1508 (+24.5%)
0.04 Antisymm	0.1188 (6) (W)	0.1116 (8) (−6.1%)	0.1241 (7) (+4.5%)	0.1280 (9) (+7.7%)	0.1201 (+1.1%)
0.05 Antisymm	0.1027 (1) (GL)	0.1136 (6) (+10.6%)	0.1262 (6) (+22.9%)	0.1302 (7) (+26.8%)	0.1006 (−2.0%)

For ν_f=0.35 (the value used for the isotropic results), the factor before the moduli product term becomes 0.862, which, when compared with the value 0.91 of the Hoff and Mautner [1] formula, would give a critical load 5.3% lower. For the orthotropic face sheet with ν_f=0.26, the factor becomes 0.844, which would give a critical load 7.2% lower than the Hoff and Mautner [1] formula.

A few recent related studies will be mentioned at this point. Vonach and Rammerstorfer [17] have also addressed the problem of wrinkling of orthotropic sandwich plates under general loading. They tackle the problem by assuming the core to be infinitely thick and transversely isotropic and the wrinkling wave at the interface between the face sheet and the core to be sinusoidal. Thereafter they are able to solve the governing differential equation (based on plate theory) describing the face sheets deformation. Another related study is that by Grenestedt and Olsson [18], which assumes two layers of different materials attached to a semi-infinite substrate of a third material and treats the problem from an elasticity theory. These studies make in general less restrictive assumptions than the old formulas and utilize more advanced methods of analysis but, nevertheless, they still do not correspond to the configuration of a finitely thick core between two finitely thick face sheets, which is studied in this paper.

As far as global buckling, the Euler load is simply

$$P_{Eul}=\frac{\pi^2(EI)_{eq}}{L^2}\quad (EI)_{eq}=2w\left[E_f\frac{f^3}{12}+E_ff\left(\frac{f}{2}+c\right)^2+E_c\frac{c^3}{3}\right]. \tag{12a}$$

A formula correcting for transverse shear is in Allen's book [4] as follows:

$$P_{gl}=\frac{P_E}{1+[P_E2c/G_cw(2c+f)^2]};\quad P_E=E_fwf(2c+f)^2\frac{\pi^2}{2L^2}. \tag{12b}$$

Results are produced for the following configuration: L/h=5 where h=2(f+c) is the total plate thickness and f/h=0.01 to 0.05 (we also assigned the width w/L=2).

First, the case of both faces being isotropic, is examined. Therefore, we first consider isotropic phases, E_f/E_c=1000 and 500, ν_f=0.35 and ν_c=0.

Table 1 shows the critical load for E_f/E_c=1,000 and Table 2 for E_f/E_c=500. Before discussing the results, it should be noticed that these results have been derived for the isotropic phases with ν_c=0, because this has been historically emphasized.

In general, we can make the following conclusions for the isotropic case:

(1) The Goodier and Neou [2] formula is the most accurate; next in accuracy is Hoff and Mautner [1]. In both cases the accuracy is improved for the thinner face sheets, i.e., for the smaller f/h ratios.
(2) For the cases considered where wrinkling dominates, the Goodier and Neou [2] formula is within 5% of the elasticity value.
(3) For the cases considered, and whenever global buckling dominates, the Allen's global buckling formula [4] which corrects for transverse shear, performs very well, being within 2% of the elasticity critical load.
(4) It is possible that the global buckling load is less than the wrinkling formulas, as in the case of E_f/E_c=500, f/h=0.04, in which P^{GL}_{Allen} is less than $P^{W}_{Goodier}$; yet wrinkling dominates according to the elasticity solution. Although the exact mode of buckling may not be the most important issue, this indicates the complexity and the difficulty of drawing the right conclusions when only simple formulas are employed.
(5) Allen's [4] formula is conservative whenever wrinkling dominates. On the contrary, Hoff and Mautner's [1] formula is non-conservative whenever wrinkling dominates. But the amount of non-conservatism is quite moderate.
(6) Whenever global buckling dominates, Allen's [4] formula which corrects the Euler load for transverse shear, is conservative.
(7) Whenever global buckling dominates, the critical load being only 5%–10% of the Euler load (w/o shear) indicates the very strong influence of transverse shear effects on sandwich buckling.
(8) Antisymmetric buckling seems to dominate in the cases considered.

Next, the case of either or both phases being orthotropic is examined.

Table 3 gives results for E-glass/polyester unidirectional facings and R75 cross-linked PVC foam core. E-glass/polyester facings moduli are (in GPa): E_1^f=40, E_2^f=E_3^f=10, G_{23}^f=3.5, G_{12}^f=G_{31}^f=4.5; and the facings Poisson's ratios: ν_{12}^f=0.26, ν_{23}^f=0.40, and ν_{31}^f=0.065. The PVC core is isotropic with modulus E^c=0.075 GPa and Poisson's ratio ν^c=0.30.

Since the axial modulus ratio of the facings and the core is close to 500, the results of Table 3 can be compared with the results of Table 1. In Table 3, the facings are orthotropic rather than isotropic and the core, although isotropic, does not have zero Poisson's ratio. We can conclude that:

Table 3 Critical loads for E-glass/polyester faces and PVC/R75 foam core. Loads normalized with the Euler load (w/o shear), Eq. (12a) W=wrinkling (multi-wave); GL=global (Euler)

f/h	$\tilde{P}_{Elast}$ (m)	$\tilde{P}^W_{Allen}$ (m)	$\tilde{P}^W_{Goodier}$ (m)	$\tilde{P}^W_{Hoff}$ (m)	$\tilde{P}^{GL}_{Allen}$
	(% difference from Elasticity)				
0.01	0.1023	0.09454	0.1165	0.1103	0.2636
Antisymm	(30) (W)	(30)	(28)	(32)	
		(−7.6%)	(+13.9%)	(+7.8%)	(+157.7%)
0.02	0.1012	0.09375	0.1155	0.1093	0.1576
Antisymm	(15) (W)	(15)	(14)	(16)	
		(−7.4%)	(+14.1%)	(+8.0%)	(+55.7%)
0.03	0.1008	0.09473	0.1167	0.1105	0.1136
Antisymm	(9) (W)	(10)	(9)	(11)	
		(−6.0%)	(+15.8%)	(+9.6%)	(+12.7%)
0.04	0.09096	0.09620	0.1185	0.1122	0.08967
Antisymm	(1) (GL)	(7)	(7)	(8)	
		(+5.8%)	(+30.3%)	(+23.4%)	(−1.4%)
0.05	0.07596	0.09790	0.1206	0.1142	0.07464
Antisymm	(1) (GL)	(6)	(6)	(6)	
		(+28.9%)	(+58.8%)	(+50.3%)	(−1.7%)

(9) The Goodier and Neou [2] formula no longer exhibits the excellent accuracy that was shown in Table 1. Notice, though, that this formula was derived for isotropic phases with $\nu_c=0$. In fact, in Table 3, this formula has the worst performance although in Table 1 it had the best performance whenever wrinkling occurred.

(10) Allen's [4] formula is still conservative whenever wrinkling dominates. On the contrary, all other wrinkling formulas are non-conservative (again, whenever wrinkling dominates).

(11) Global buckling occurs sooner now, even for $f/h=0.04$.

(12) Whenever global buckling dominates, Allen's [4] formula, which corrects the Euler load for transverse shear, is still conservative.

Table 4 gives results for graphite/epoxy unidirectional facings and hexagonal glass/phenolic honeycomb core. The graphite/epoxy facings moduli are (in GPa): $E_1^f=181, E_2^f=E_3^f=10.3, G_{23}^f=5.96, G_{12}^f=G_{31}^f=7.17$; and the facings Poisson's ratios: $\nu_{12}^f=0.28, \nu_{23}^f=0.49$, and $\nu_{31}^f=0.0159$. The honeycomb core moduli are (in GPa): $E_1^c=E_2^c=0.032, E_3^c=0.390, G_{23}^c=G_{31}^c=0.048, G_{12}^c=0.013$; and the core Poisson's ratios: $\nu_{31}^c=\nu_{32}^c=\nu_{21}^c=0.25$.

Table 4 Critical loads for graphite/epoxy faces and glass/phenolic honeycomb core. Loads normalized with the Euler load (w/o shear), Eq. (12a) W=wrinkling (multi-wave); GL=global (Euler).

f/h	$\tilde{P}_{Elast}$ (m)	$\tilde{P}^W_{Allen}$ (m)	$\tilde{P}^W_{Goodier}$ (m)	$\tilde{P}^W_{Hoff}$ (m)	$\tilde{P}^{GL}_{Allen}$
	(% difference from Elasticity)				
0.01	0.07037	0.01884	0.02209	0.02196	0.03517
Antisymm	(26) (W)	(14)	(13)	(15)	
		(−73.2%)	(−68.6%)	(−68.8%)	(−50.0%)
0.02	0.06552	0.01917	0.02247	0.02234	0.01826
Antisymm	(1) (GL)	(7)	(6)	(7)	
		(−70.7%)	(−65.7%)	(−65.9%)	(−72.1%)
0.03	0.04576	0.01955	0.02291	0.02278	0.01253
Antisymm	(1) (GL)	(5)	(4)	(5)	
		(−57.3%)	(−49.9%)	(−50.2%)	(−72.6%)
0.04	0.03577	0.01994	0.02337	0.02324	0.00963
Antisymm	(1) (GL)	(3)	(3)	(4)	
		(−44.3%)	(−34.7%)	(−35.0%)	(−73.1%)
0.05	0.02988	0.02035	0.02385	0.02372	0.00789
Antisymm	(1) (GL)	(3)	(3)	(3)	
		(−31.9%)	(−20.2%)	(−20.6%)	(−73.6%)

In this case the axial modulus ratio of the facings and the core is very large, close to 5,000. Notice also that in Table 4 both facings and the core are orthotropic. The results show clearly the inadequacy of the simple wrinkling formulas and even the global buckling formula whenever a strongly orthotropic construction is made. In particular we can conclude that:

(13) Global buckling occurs even sooner now, even for $f/h=0.02$. Actually, only in the $f/h=0.01$ case, wrinkling dominates.

(14) All formulas are strongly conservative. Whenever global buckling dominates, Allen's [4] formula shows a very large degree of conservatism, being almost one quarter of the elasticity critical load. The same is true whenever wrinkling dominates, the wrinkling formulas show a very large degree of conservatism, being almost a quarter of the elasticity critical wrinkling load.

The thickness-wise variation of the displacements has been a matter of great interest. Hoff and Mautner [1] based their analysis on a linear decay of the transverse displacement, $W(z)$, whereas Plantema [16] based his analysis on an exponential decay. Figure 3(a) shows the transverse displacement, $W(z)$ and Fig. 3(b) shows the axial displacement, $U(z)$, for the two cases of isotropic phases, $f/h=0.02$ and at the critical point. Since the modes are derived by setting the core displacement at the middle, $W_c=1$, the displacements are normalized with the corresponding mid-point ($z=0$) transverse displacement of the core, W_{c0}. We see that the variation is certainly nonlinear through the core in both $W(z)$ and $U(z)$. The $W(z)$ has a high slope gradient near the core mid-line, $z=0$.

Figures 4(a) and 4(b) show the same displacements for the two cases of orthotropic phases examined and $f/h=0.01$ and at the critical point. Double y-axis plots were used in this case because the scales for the two material systems are very much apart. The displacements are again normalized with the corresponding mid-point ($z=0$) transverse displacement of the core, W_{c0}. We see that, again, the variation is nonlinear through the core, in both $W(z)$ and $U(z)$ and the $W(z)$ has again a high slope gradient near the core mid-line, $z=0$. A comparison of the isotropic and the orthotropic plots shows that the nonlinearities are more pronounced in the latter case.

A literature search has not revealed detailed finite element data on the wrinkling of sandwich plates (based on solid elements), which can be used to compare with the present solution. This indicates that there is a need for numerical studies of wrinkling, based on various finite element (or other numerical) formulations. In this regard, the present elasticity solution will serve to compare the accuracy of the various numerical approaches. We can, however, obtain a validation of the solution developed in this paper by comparing with the early buckling experiments performed in 1945 by Hoff and Mautner [1]. In these experiments, the face sheet material was a high strength paper plastic (papreg, isotropic with Young's modulus 3×10^6 lb per in.^{2}). The sandwich specimens had a cellular acetate core, also isotropic with Young's modulus 1,500 lb per in.^{2} (for both the face sheet and the core, the Poisson's ratio used in the analysis was 0.30). The length of all the specimens in the direction of the applied load, L, was 10.5 in. The width of the specimens perpendicular to the direction of the applied load, w, varied as well as the thickness of the face sheet and that of the core. Table 5 shows the critical load, as predicted from Hoff's formula (Eq. (11d)) and from the present elasticity formulation for the observed mode of buckling. We can conclude that, in general, the present elasticity solution predicts loads closer to the experimentally measured values. In some cases, where the critical half-wave numbers, m, are high and close to each other, the elasticity and the Hoff's solution do not differ practically (as in the third and fourth cases in Table 5). In other cases, the Hoff's solution would be very non-conservative (as in the fifth and seventh cases in Table 5) and it would predict wrinkling at half-wave

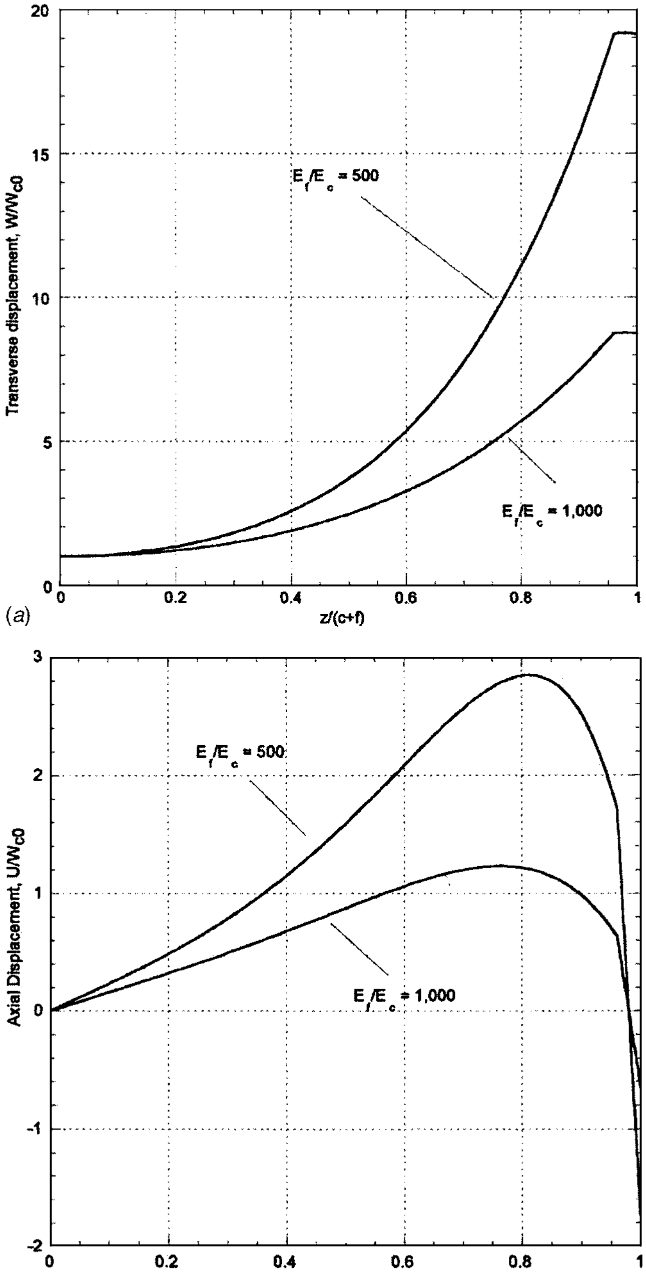

Fig. 3 (*a*) **Thickness-wise variation of the transverse displacement, W, for isotropic phases and $f/h=0.02$ (at the critical point). The displacement is normalized with the mid-point ($z=0$) transverse displacement of the core, W_{c0}. (*b*) Thickness-wise variation of the axial displacement, U, for isotropic phases and $f/h=0.02$ (at the critical point). The displacement is normalized with the mid-point ($z=0$) transverse displacement of the core, W_{c0}.**

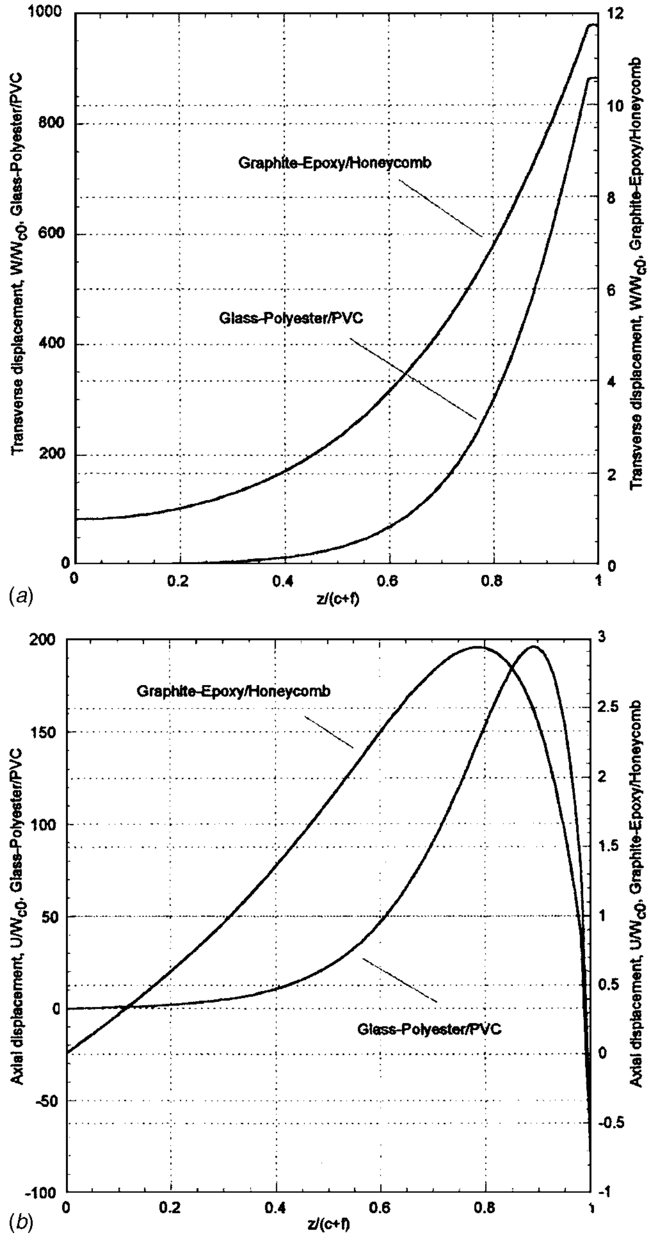

Fig. 4 (*a*) **Thickness-wise variation of the transverse displacement, W, for the orthotropic phases examined and $f/h=0.01$ (at the critical point). The displacement is normalized with the corresponding mid-point ($z=0$) transverse displacement of the core, W_{c0}. (*b*) Thickness-wise variation of the axial displacement, U, for the orthotropic phases examined and $f/h=0.01$ (at the critical point). The displacement is normalized with the corresponding mid-point ($z=0$) transverse displacement of the core, W_{c0}.**

numbers, m, which are much higher than the elasticity solution; the latter being much closer to the experiments. Note that Hoff and Mautner's paper [1] does not report data on the experimental half wave numbers. The data in Table 5 can be considered as offering a validation of the accuracy of the present solution.

The intent of this study was to focus on the wrinkling behavior of sandwich beams (or wide plates), hence the illustrative examples were for very thin facings. Future elasticity studies will focus on the global buckling behavior which is expected to dominate with thicker facings.

4 Conclusions

An elasticity solution to the problem of buckling of sandwich beams or wide sandwich panels subjected to axially compressive loading is presented. A symmetric section is considered with all constituent phases, i.e., the facings and the core, being in general orthotropic. For the configurations considered with both phases isotropic, the Goodier and Neou [2] wrinkling formula is the most accurate, next in accuracy being the Hoff and Mautner [1] and in both cases the accuracy improved for the thinner face sheets. Furthermore, whenever wrinkling dominates, Allen's [4] formula is always conservative but the Hoff and Mautner's [1] wrinkling

Table 5 Comparison with experimental data from Hoff and Mautner [1]

Width, thick ness, w (in.)	Face thick ness, f (in.)	Core thick ness, $2c$ (in.)	Observed mode of buckling	Critical load lb from Hoff Eq. (11d) (m)	Critical load lb from present elasticity (m)	Buckling load lb from experiments (Hoff and Mautner [1])
4	0.02025	0.441	Sym	2035.8 (21)	2273.9 (24)	2240
4	0.02025	0.434	Sym	2035.7 (21)	2284.5 (24)	2220
4	0.00675	0.458	Sym	686.4 (64)	690.7 (60)	750
4	0.00675	0.448	Sym	686.1 (64)	690.4 (60)	700
11	0.02025	0.230	Anti-Sym	5584.1 (21)	1079.3 (1)	1600
4	0.01125	0.725	Sym	1143.0 (38)	1150.2 (36)	1455
4	0.01125	0.076	Anti-Sym	1126.8 (38)	435.4 (1)	350

formula is slightly non-conservative. Whenever global buckling dominates, Allen's [4] global buckling formula, which corrects the Euler load for transverse shear, is conservative and moreover, the critical load is only 5%–10% of the Euler load (w/o shear), indicating the very strong influence of transverse shear effects on sandwich buckling. Antisymmetric buckling seems to be dominant in the cases considered. With the ortotropic (rather than isotropic) phases examined, wrinkling is harder to occur, global buckling taking place for even thinner face sheets. But now the accuracy of the simple wrinkling and global buckling formulas is seriously compromised, and there are large deviations from the elasticity solution. In particular, for the graphite/epoxy facings and glass/phenolic honeycomb core, whenever global buckling dominates, Allen's [4] global buckling formula shows a very large degree of conservatism, being almost one quarter of the elasticity critical load. The same is true for this material system whenever wrinkling dominates, the simple wrinkling formulas show a very large degree of conservatism, being almost a quarter of the elasticity critical wrinkling load. In addition, the results show that the variation of both the transverse and axial displacement through the core is nonlinear, more so with the orthotropic phases, and with the transverse displacement exhibiting a high slope gradient near the core mid-line. The solution presented herein provides a means of accurately assessing the limitations of simplifying analyses in predicting wrinkling and global buckling in wide sandwich panels/beams.

Acknowledgment

Financial support of the Office of Naval Research, Ship Structures and Systems, S& T Division, Grant Nos. N00014-90-J-1995 and N00014-0010323, and the interest and encouragement of the Grant Monitor, Dr. Y.D.S. Rajapakse, are both gratefully acknowledged.

References

[1] Hoff, N. J., and Mautner, S. F., 1945, "The Buckling of Sandwich-Type Panels," J. Aeronaut. Sci., **12**, pp. 285–297.

[2] Goodier J. N., and Neou I. M., 1951, "The Evaluation of Theoretical Compression in Sandwich Plates," J. Aeronaut. Sci., **18**, pp. 649–657.

[3] Gough, G. S., Elam, C. F., and de Bruyne, N. A., 1940, "The Stabilization of a Thin Sheet by a Continuous Supporting Medium," J. R. Aeronaut. Soc., **44**, pp. 12–43.

[4] Allen, H. G., 1969, *Analysis and Design of Structural Sandwich Panels*, Pergamon, Oxford, UK, Chap. 8.

[5] Birman, V., and Bert, C. W., 2002, "Wrinkling of Composite-Facing Sandwich Panels Under Biaxial Loading," IMECE 02, the 2002 International Mechanical Engineering Congress & Exposition, November 17–22, New Orleans, LA.

[6] Kardomateas, G. A., 1993, "Buckling of Thick Orthotropic Cylindrical Shells Under External Pressure," ASME J. Appl. Mech., **60**, pp. 195–202.

[7] Kardomateas, G. A., and Chung, C. B., 1994, "Buckling of Thick Orthotropic Cylindrical Shells Under External Pressure Based on Non-Planar Equilibrium Modes," Int. J. Solids Struct. **31**, pp. 2195–2210.

[8] Kardomateas, G. A., 1993, "Stability Loss in Thick Transversely Isotropic Cylindrical Shells Under Axial Compression," ASME J. Appl. Mech., **60**, pp. 506–513.

[9] Kardomateas, G. A., 1995, "Bifurcation of Equilibrium in Thick Orthotropic Cylindrical Shells Under Axial Compression," ASME J. Appl. Mech., **62**, pp. 43–52.

[10] Soldatos, K. P., and Ye, J-Q., 1994, "Three-Dimensional Static, Dynamic, Thermoelastic and Buckling Analysis of Homogeneous and Laminated Composite Cylinders," Compos. Struct., **29**, pp. 131-143.

[11] Kardomateas, G. A., and Simitses, G. J., 2005, "Elasticity Solution for the Bucking of Long Sandwich Cylindrical Shells Under External Pressure," ASME J. Appl. Mech., **72**, pp. 493–499.

[12] Lekhnitskii, S. G., 1963, *Theory of Elasticity of an Anisotropic Elastic Body*, Holden Day, San Francisco (also Mir Publishers, Moscow, 1981).

[13] Kardomateas, G. A., 2001, "Elasticity Solutions for a Sandwich Orthotropic Cylindrical Shell Under External Pressure, Internal Pressure and Axial Force," AIAA J. **39**, pp. 713–719.

[14] Novozhilov, V. V., 1953, *Foundations of the Nonlinear Theory of Elasticity*, Graylock, Rochester, NY.

[15] Press, W. H., Flannery, B. P., Teukolsky, S. A., and Vetterling, W. T., 1989, *Numerical Recipes*, Cambridge University Press, Cambridge.

[16] Plantema, F. J., 1966, *Sandwich Construction*, John Wiley & Sons, New York.

[17] Vonach, W. K., and Rammerstorfer, F. G., 2000, "Wrinkling of Thick Orthotropic Sandwich Plates under General Loading Conditions," Arch. Appl. Mech. **70**, pp. 338–348.

[18] Grenestedt, J. L., and Olsson, K.-A., 1995, *Proc., Third International Conference on Sandwich Construction*, Southampton, U.K., 12–15 September.